fermentation

MDPI

Article

Autoinducer-2: Its Role in Biofilm Formation and L-Threonine Production in *Escherichia coli*

Hui Han [1,2], Kaijie Zhang [1,2], Guoxiong Li [1,2], Ying Yu [1,2], Shuqi Shi [1,2], Caice Liang [1,2], Huanqing Niu [1,2], Wei Zhuang [1,2], Dong Liu [1,2], Pengpeng Yang [1,2], Tianpeng Chen [1,2,*], Wenjun Sun [1,2,*] and Yong Chen [1,2]

1 National Engineering Research Center for Biotechnology, College of Biotechnology and Pharmaceutical Engineering, Nanjing Tech University, Nanjing 211816, China; hanhui@njtech.edu.cn (H.H.); huanqingniu@njtech.edu.cn (H.N.); weizhuang@njtech.edu.cn (W.Z.); liudong@njtech.edu.cn (D.L.); yang-pengpeng@njtech.edu.cn (P.Y.); chenyong1982@njtech.edu.cn (Y.C.)

2 State Key Laboratory of Materials-Oriented Chemical Engineering, College of Biotechnology and Pharmaceutical Engineering, Nanjing Tech University, Nanjing 211816, China

* Correspondence: chentianpeng@njtech.edu.cn (T.C.); sunwenjun@njtech.edu.cn (W.S.); Tel.: +86-25-86990001 (W.S.); Fax: +86-25-58139389 (W.S.)

Abstract: Biofilms enable bacterial cells to adhere and thrive on surfaces, with associated changes in growth and gene expression aiding their survival in challenging environments. While previous research has explored *E. coli* biofilm formation, there has been limited exploration of its application in industrial production. Prior studies have shown that immobilized fermentation can enhance L-threonine production. This study aims to augment biofilm formation and subsequently increase L-threonine production in *E. coli* by regulating the quorum sensing system, focusing on key AI-2-related genes, including *luxS*, *lsrB*, *lsrK*, and *lsrR*. In +pluxS and +plsrB strains, AI-2 levels were significantly altered, resulting in enhanced biofilm formation, increased curli expression, shorter free-cell fermentation periods, and improved production efficiency through immobilized continuous fermentation. In a single batch of free-cell fermentation with *E. coli* W1688, L-threonine production was 10.16 g/L. However, +pluxS and +plsrB strains achieved L-threonine yields of 15.27 g/L and 13.38 g/L, respectively, after seven fermentation batches. Additionally, the fermentation period was reduced from 36 h to 28 h and 30 h, respectively.

Keywords: *Escherichia coli*; AI-2; *luxS*; *lsrB*; biofilm; L-threonine

check for updates

Citation: Han, H.; Zhang, K.; Li, G.; Yu, Y.; Shi, S.; Liang, C.; Niu, H.; Zhuang, W.; Liu, D.; Yang, P.; et al. Autoinducer-2: Its Role in Biofilm Formation and L-Threonine Production in *Escherichia coli*. *Fermentation* **2023**, *9*, 916. https://doi.org/10.3390/fermentation9100916

Academic Editor: Lei Chen

Received: 18 September 2023
Revised: 8 October 2023
Accepted: 11 October 2023
Published: 19 October 2023

1. Introduction

Biofilms are microbial communities that can adhere to biotic and abiotic surfaces by secreting extracellular polymers to enhance adhesion and aggregation [1]. Compared to cells in planktonic state, cells in biofilms exhibit a higher colonization capacity and tolerance to exogenous stress [2]. Biofilms are medically important because they are involved in many bacterial infections [3]. For example, *Escherichia coli* (*E. coli*) biofilm is the major causative agent for recurrent urinary tract infections [4], and *Staphylococcus aureus* can form biofilms on the surface of medical devices and host tissues, which is the main reason for the persistence of chronic infections [5]. However, biofilms are also beneficial in several fields, including drinking water filtration, wastewater and solid waste treatment, biochemical production etc. [6]. A variety of microorganisms are present in biofilms that can absorb organic matter and pollutants. Additionally, biofilm-based fermentation performs well, with high production and efficiency, with its inherent self-fixation ability, strong resistance to adverse environments [7], and the long-term maintenance of cell activity [8]. The biofilms of industrial strains, such as *Saccharomyces cerevisiae*, *Aspergillus niger*, *E. coli*, and *Clostridium acetobutylicum*, have been applied to produce biochemical products effectively [9–11].

L-threonine, one of the eight essential amino acids, has found wide applications in food, feed, medicine, and other fields. Currently, the industrial production of L-threonine

primarily relies on free-cell fermentation. *E. coli* is the primary strain for L-threonine production due to its well-defined genetic background and shorter fermentation period [12]. Nevertheless, as fermentation progresses, the recessions of cell proliferation and differentiation gradually become more serious in the industrial environment. This leads to the synthesis of by-products, accumulation of waste and a low conversion rate. The continuous (repeated-batch) fermentation of *E. coli* in a biofilm reactor produces a large amount of L-threonine in a shorter fermentation period than free-cell fermentation [8].

Under natural conditions, biofilm formation by bacteria occurs in three distinct stages: attachment, maturation, and disintegration [13]. Biofilm formation is influenced by various external (such as pH, temperature, nutrients, and metal ions) and internal factors (quorum sensing (QS) molecules) [14–16]. The QS system is a cell-to-cell communication mechanism that controls the expression of genes in various cellular processes [17], such as virulence, luminescence, motility, sporulation, and especially biofilm formation [18,19]. Three main QS systems have been reported: autoinducing peptide (AIP) QS system in Gram-positive bacteria, acyl-homoserine lactone (AHL) QS system in Gram-negative bacteria, and autoinducer-2 (AI-2) QS system in both Gram-negative and Gram-positive bacteria [20–22].

Among the bacteria that use AI-2 as a signal molecule, *E. coli* has attracted the attention of genetic engineering research since the QS system in *E. coli* has been well characterized [23–26]. The signal molecule AI-2 is produced by the LuxS protein, an enzyme involved in the activated methyl cycle (AMC) [26]. In AMC, LuxS cleaves S-ribosylhomocysteine (SRH) to yield homocysteine and 4,5-dihydroxy-2,3-pentanedione that subsequently rearranges into AI-2 [27]. Then, AI-2 is exported by the membrane proteins and accumulates in the extracellular space. With the increase in concentration of AI-2 during the exponential phase of growth, AI-2 is imported by the transporter LsrACDB and then phosphorylated (AI-2-P) by the kinase LsrK. The AI-2-P binds to repressor protein LsrR and relieves repression of the *lsr* operon, resulting in additional transcription of AI-2 uptake and processing genes [28].

Previous studies have highlighted the importance of AI-2 dynamics on the *E. coli* QS system, including AI-2 synthesis, uptake, and phosphorylation, and its role in *lsr* operon expression [29]. However, limited studies are available on how the AI-2 QS system affects biofilm formation in *E. coli*. In this study, we examined the effects of modifying the four key genes (*luxS*, *lsrB*, *lsrK* and *lsrR*) in the AI-2 QS system on the biofilm formation of *E. coli* W1668. Changes in the gene expression were verified using quantitative real-time polymerase chain reaction (qRT-PCR). We demonstrated that overexpression of *luxS* and *lsrB* enhanced the biofilm formation of *E. coli* W1668 by upregulating genes that control curli synthesis. Likewise, the fermentation ability of mutants to produce L-threonine was examined, and a biofilm-based immobilized fermentation was constructed. Overall, this study presents a successful development case of transforming *E. coli* biofilm formation mediated by AI-2 QS system into an immobilized continuous fermentation system for the production of L-threonine.

2. Results

2.1. Growth of luxS, lsrB, lsrK, and lsrR Mutants

To determine whether the deletion or overexpression of the four key genes (*luxS*, *lsrB*, *lsrK* and *lsrR*) in an AI-2 QS system influence the growth of *E. coli* W1688 [30], we generated strains ΔluxS, ΔlsrB, ΔlsrK, ΔlsrR, +pluxS, +plsrB, +plsrK, and +plsrR and evaluated their bacterial growth by measuring OD_{600} from 2 to 14 h. All mutants, including the deletion and overexpression of the key genes, showed a comparable growth rate to that of *E. coli* W1688 (Figure 1A,B). These results suggest that the deletion or overexpression of the four key genes has no significant effect on the growth of *E. coli* W1688.

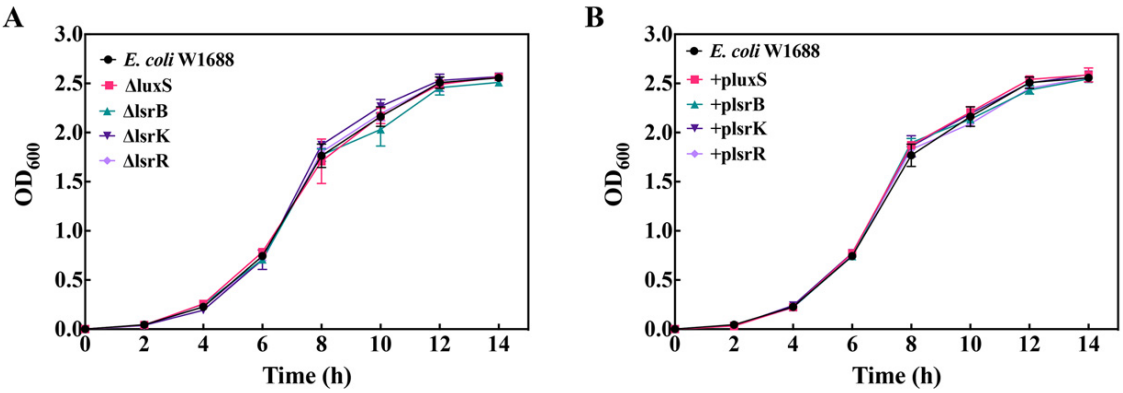

Figure 1. Growth curves of *E. coli* W1688 and (**A**) deletion and (**B**) overexpression mutants. The cell densities were determined by measuring OD600 at 2, 4, 6, 8, 10, 12, and 14 h.

2.2. lsrB, luxS, lsrK, and lsrR affect biofilm formation in E. coli W1688

Since the AI-2 QS plays a significant role in the biofilm formation of many bacteria [31], the ability of *E. coli* W1688 and its mutants to form biofilm was also determined. As shown in Figure 2A, there were no significant differences between ΔlsrK, ΔlsrR, and +plsrK compared with *E. coli* W1688. The biofilm formation of ΔluxS and ΔlsrB decreased by 38% and 30%, respectively, while +pluxS and +plsrB displayed enhanced biofilm formation by 21% and 31%, respectively. Moreover, we observed a 33% reduction in the biofilm formation of +plsrR. The morphotypes of +pluxS and +plsrB were dry and rough, and appeared deeper pink on YESCA-CR plates as compared than *E. coli* W1688 and other mutants (Figure 2B), indicating increased curli fibre and biofilm formation.

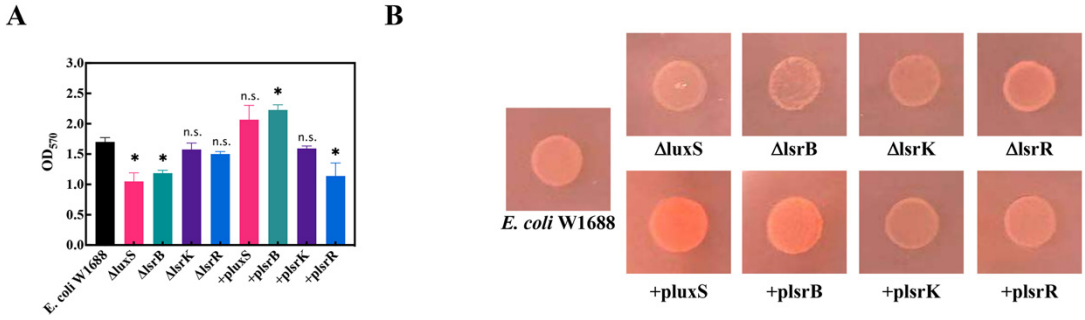

Figure 2. Ability to form biofilm and curli of *E. coli* W1688 and all mutants. (**A**) All strains were incubated in 96-well plates and subjected to CV staining assay. Absorbance at 570 nm was measured using a microplate reader. (**B**) All strains were inoculated on YESCA-CR plates. The colour shade of the colony combined with CR reflects the curli forming ability. p values were computed using Student's t test (n.s., not significant at $p > 0.05$; * $p < 0.05$).

The morphology of *E. coli* mutants was analysed using SEM to further verify their ability to form biofilms. Results showed that +pluxS and +plsrB strains displayed substantial adhesion on coverslips and formed biofilm after 30 h incubation (Figure 3A). Meanwhile, the amount of biofilm formation was slightly reduced in both ΔluxS and ΔlsrB compared to *E. coli* W1688, while the other mutants showed negligible visual differences.

DAPI is a fluorescent dye that can bind strongly to DNA [32]. Living cells in biofilms can be observed using DAPI under a fluorescence microscope. The results of DAPI staining of all mutants on the coverslips are shown in Figure 3B. *E. coli* W1688 cells were highly scattered on the coverslips, whereas obvious cell aggregates appeared in +pluxS and +plsrB strains. These results suggest that the overexpression of *luxS* or *lsrB* is beneficial to the adhesion and aggregation of *E. coli*, which contributed to the formation of biofilms. We also found that the ΔluxS and ΔlsrB cells stained by DAPI were more scattered compared to

the *E. coli* W1688 biofilm; the scattering was slightly reduced in ΔlsrK, +plsrK and +plsrR biofilms, and ΔlsrR biofilms did not show any significant change.

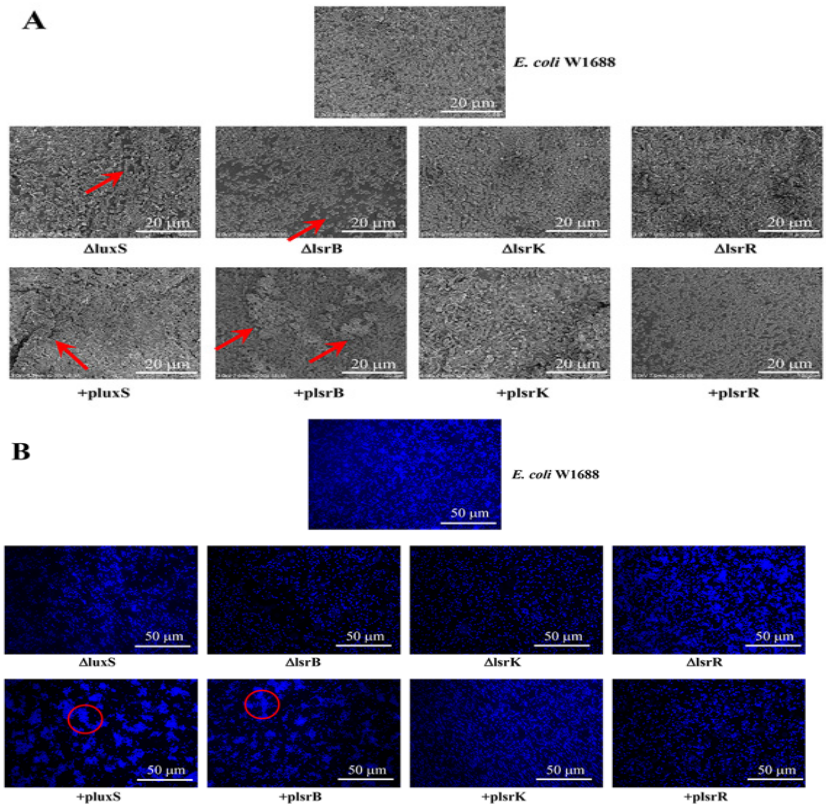

Figure 3. Biofilm formation on coverslips. (**A**) All strains were incubated in 12-well plates with round coverslips. The cells were then collected for ethanol gradient dehydration and observed using SEM. Scale bar, 20 μm. (**B**) The biofilm cells on the coverslips were stained with DAPI, and the biofilm formation state was observed with a fluorescence microscope. Scale bar, 50 μm.

To further explore the mechanism of biofilm formation, qRT-PCR was performed to determine the expression levels of the four key genes in the AI-2 QS system and *E. coli* biofilm-related genes. The deletion of *luxS*, *lsrB*, *lsrK*, and *lsrR* caused a prominent decrease in the expression levels of the CSG and FIM gene families (Figure 4). In +pluxS, the expression levels of CSG genes and FIM genes were significantly upregulated (Figure 4).

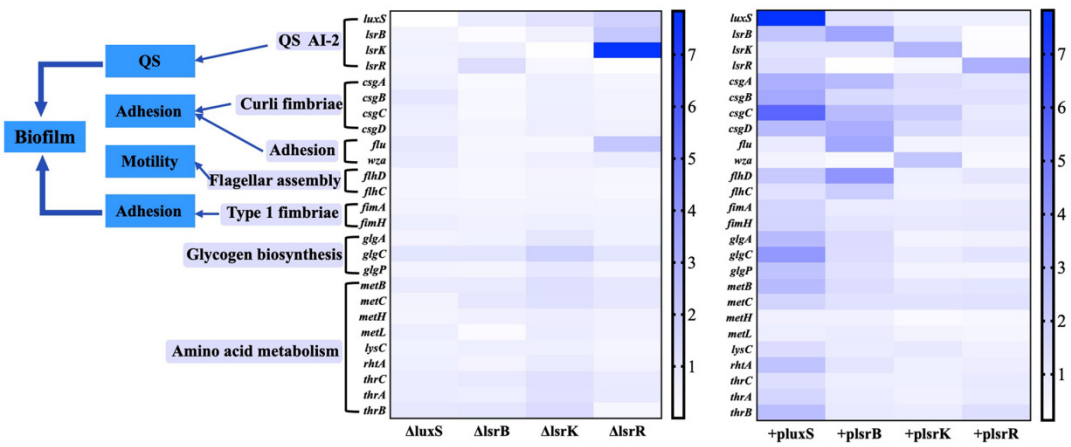

Figure 4. Biofilm-related qRT-PCR results indicating expression of genes involved in QS, adhesion, motility, and amino acid metabolism.

As the expression level of CSG family genes was significantly upregulated in +pluxS, and curli formation in *E. coli* is mediated by the CSG family, we examined the phenotypes of various mutants grown on YESCA-CR plates containing CR and brilliant blue. The increased curli fibre formation in +pluxS and +plsrB, denoted by a deeper shade of pink on the YESCA-CR plates (Figure 2B), was consistent with the increased expression of CSG family genes in these strains. Together, these results highlight that *luxS* and *lsrB* play an important role in the regulation of *E. coli* biofilm formation.

2.3. Overexpression of lsrB and luxS Affects the Motility of E. coli W1688

Effective "swarm" movement affects the colonization of *E. coli* at the initial stage of biofilm formation [33]. As shown in Figure 5A, the outer diameter of colonies formed in +pluxS and +plsrB were significantly larger than *E. coli* W1688, while those in ΔlsrK, ΔlsrR, +plsrK, and +plsrR strains were comparable to *E. coli* W1688. We further compared the diameters of the outer chemotactic ring of all mutants. The diameter of the outer chemotactic ring of *E. coli* W1688 was 1.7 cm. The rings of ΔluxS, ΔlsrB, ΔlsrB, ΔlsrB, +plsrK, and +plsrR were only slightly smaller than that of *E. coli* W1688, whereas +pluxS and +plsrB showed significant differences with outer chemotactic ring sizes of 2.9 cm and 4.1 cm, respectively.

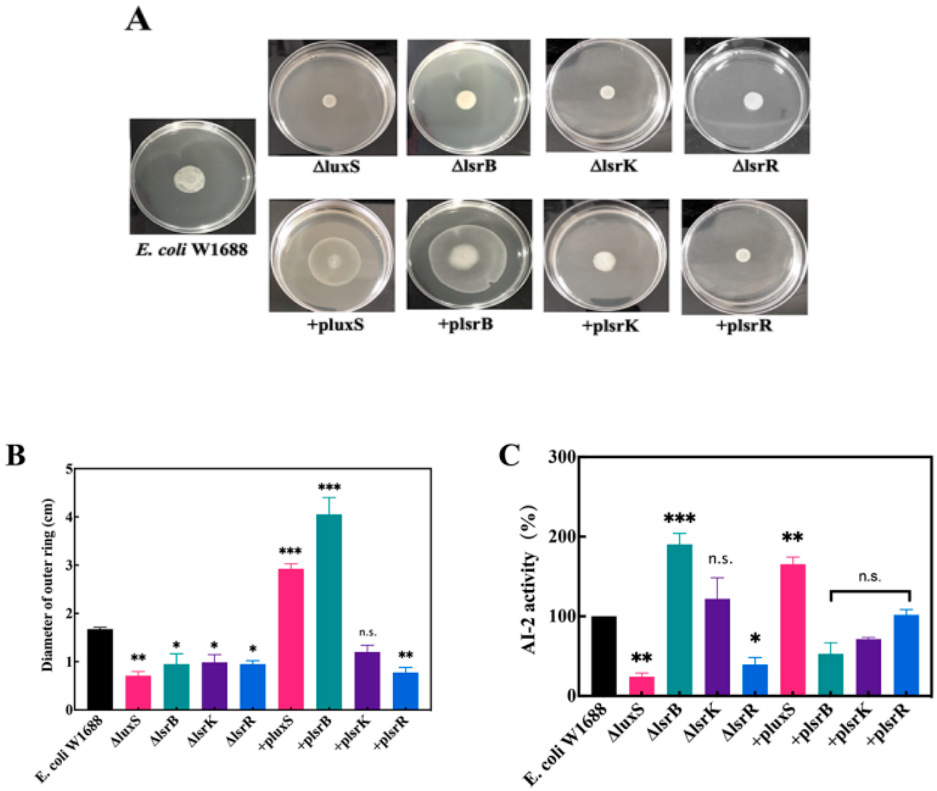

Figure 5. *E. coli* motility assay and AI-2 activity. (**A**) Chemotactic rings of *E. coli* W1688 and all mutants observed using Eiken ager plates (diameter: 7 cm). (**B**) Diameters of the outer chemotactic rings. (**C**) AI-2 activity of all strains. *p* values were computed using Student's *t* test (n.s., not significant at $p > 0.05$; *** $p < 0.001$; ** $p < 0.01$; and * $p < 0.05$).

To explore the relationship between motility and the biofilm in more detail, the transcription levels of *flhC* and *flhD*, which are the transcriptional activators of the flagellar class II operons in *E. coli*, were examined. Compared with *E. coli* W1688, both *flhC* and *flhD* had lower expression levels in ΔluxS and ΔlsrB (Figure 4). In +pluxS, the expression levels of *flhC* and *flhD* were increased by 1.3-fold and 2.1-fold, respectively, while those in +plsrB increased by 2-fold and 4.1-fold, respectively. A downward trend was observed in the other mutants. These data were consistent with the results of swarming (Figure 5A,B).

2.4. luxS and lsrB Are Necessary for AI-2 Production and Transport in E. coli W1688

LuxS is an enzyme involved in the metabolism of SRH, producing AI-2 [34]. AI-2 activity was measured in *E. coli* W1688 and its mutants to ascertain the roles of the analysed genes in AI-2 synthesis and transport. As shown in Figure 5C, compared with *E. coli* W1688 (100%), AI-2 activity increased to 165.43% in +pluxS and decreased to 24.16% in the ΔluxS mutant. The deletion of *lsrB* also promoted extracellular AI-2 activity, which increased to 190.21%. A downward trend was observed in the other mutants. These results showed that *luxS* and *lsrB* are necessary for AI-2 production or transport in *E. coli*.

2.5. Free-Cell Fermentation of luxS, lsrB, lsrK, and lsrR Mutants

E. coli W1688 and the corresponding *luxS*, *lsrB*, *lsrK* and *lsrR* mutants were subjected to free-cell fermentation to observe the production of L-threonine in each strain. As shown in Figure 6A, in a single batch of free-cell fermentation, *E. coli* W1688 showed a high production of L-threonine (10.16 g/L, fermentation period: 36 h). Unfortunately, the *luxS* mutants showed decreased L-threonine production (ΔluxS, 9.36 g/L, fermentation period: 42 h; +pluxS, 8.92 g/L, fermentation period: 30 h) compared to *E. coli* W1688. Likewise, *lsrB* mutants exhibited decreased L-threonine production (ΔlsrB, 9.12 g/L, fermentation period: 39 h; +plsrB, 8.83 g/L, fermentation period: 33 h) (Figure 6B). As shown in Figure 6C, compared to *E. coli* W1688, ΔlsrK and +plsrK showed a lower fermentation ability. ΔlsrK produced 9.32 g/L L-threonine during 36 h of fermentation, and +plsrK produced 7.67 g/L L-threonine during 42 h. As expected, *lsrR* also did not show significant L-threonine production (ΔlsrR, 7.45 g/L, fermentation period: 36 h; +plsR, 7.89 g/L, fermentation period: 42 h) (Figure 6D).

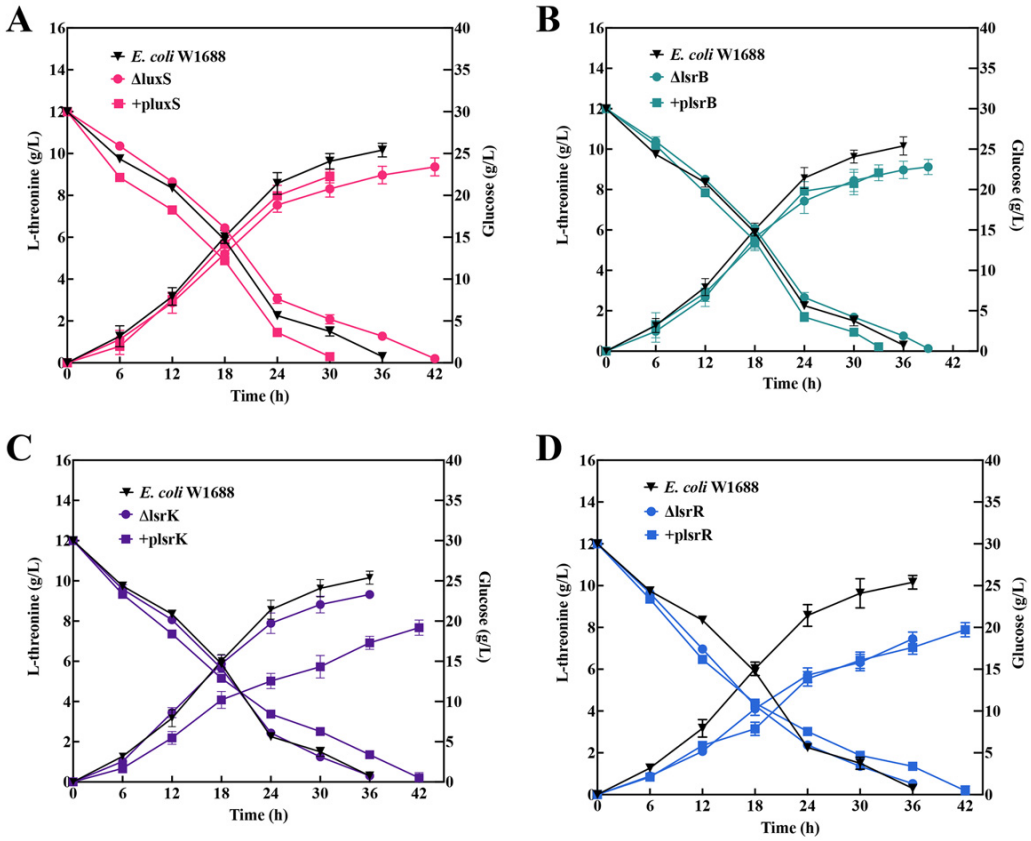

Figure 6. L-threonine production and glucose consumption in free-cell fermentation by *E. coli* W1688 and all mutants. Free-cell fermentation result of (**A**) *luxS* mutants, (**B**) *lsrB* mutants, (**C**) *lsrK* mutants, and (**D**) *lsrR* mutants.

2.6. qRT-PCR Analysis of the Free-Cell Fermentation of luxS, lsrB, lsrK, and lsrR Mutants

To examine the free-cell fermentation results of all strains, qRT-PCR was used to analyse the expression levels of the key genes related to biofilm and L-threonine metabolism (Figure 4). Figure 7 shows a schematic diagram of the genes and steps involved in the regulation of biofilm formation and L-threonine metabolism by *E. coli* AI-2 QS.

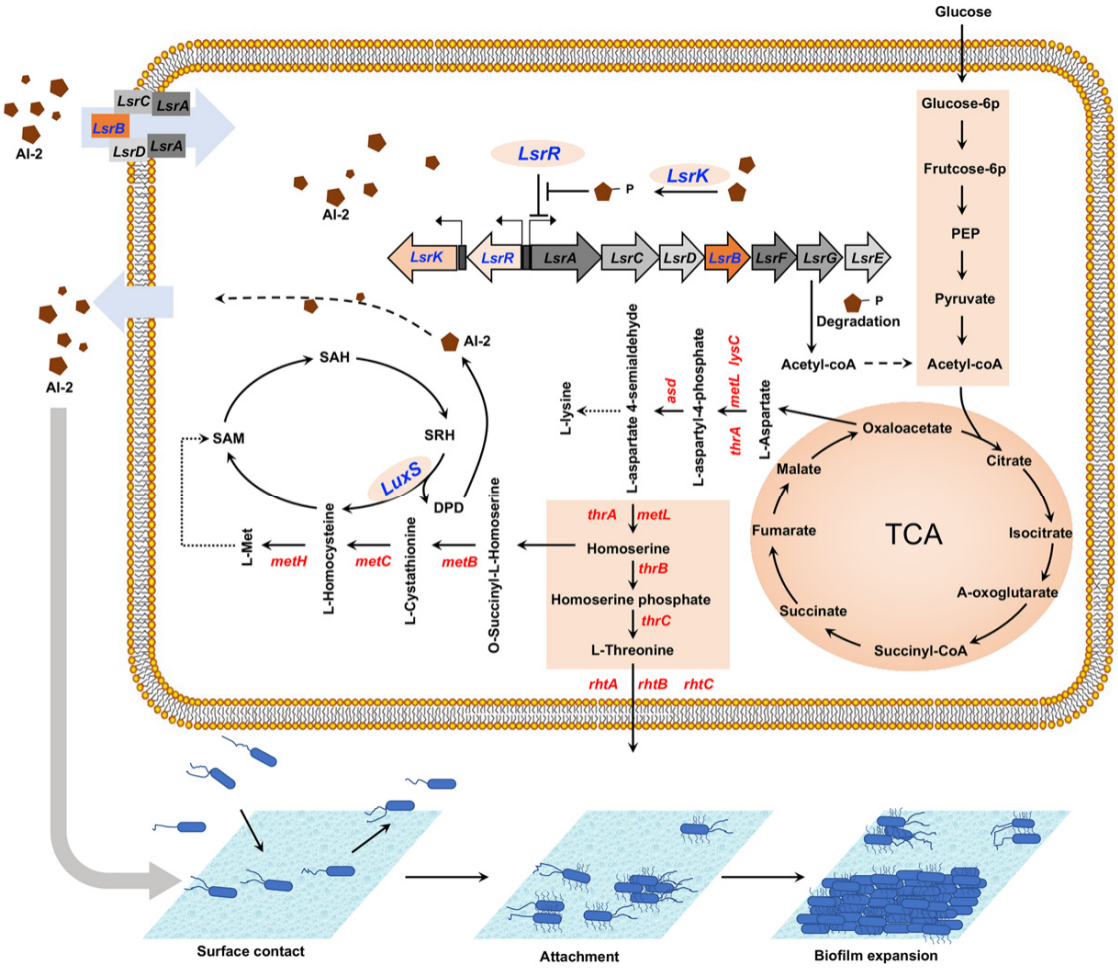

Figure 7. Schematic diagram of AI-2 QS-mediated regulation of *E. coli* W1688 biofilm formation and L-threonine metabolism.

In the +pluxS strain, the expression of three glycogen synthases, *glgA*, *glgC*, and *glgP*, were upregulated by 2.7-fold, 4-fold, and 2.4-fold, respectively. The CSG family genes encoding curli and the FIM family genes encoding type I fimbriae were also upregulated (*csgA* 3.1-fold, *csgB* 3.3-fold, *csgC* 5.6-fold, *csgD* 2.7-fold, *fimA* 1.7-fold, *fimH* 1.7-fold). Likewise, *metB* and *metC*, which are related to methionine metabolism, were also upregulated by 2.7-fold and 1.7-fold, respectively. In addition, *thrA*, *thrB*, and *thrC*, which are associated with L-threonine transport to the extracellular compartment, were also slightly upregulated (1.4-fold, 1.7-fold, and 2.6-fold, respectively). The higher expression of glycogen synthase suggested a faster rate of glucose utilization and a shorter fermentation period. However, the upregulation of genes related to curli fibres and type I fimbriae resulted in higher biofilm formation in the +pluxS strain, which also consumed a lot of the carbon source. This observation may support the reduction in L-threonine production in +pluxS compared to *E. coli* W1688. Furthermore, all genes mentioned above were downregulated in ΔluxS, leading to lower rates of glycogen synthesis, longer fermentation periods, and the reduced consumption of other carbon sources, thereby decreasing the production of L-threonine compared to *E. coli* W1688.

In the +plsrB strain, the expression of CSG/FIM gene families were upregulated (*csgA*, 3.1-fold; *csgB*, 3.3-fold; *csgC*, 5.6-fold; *csgD*, 2.7-fold; *fimA*, 1.7-fold; *fimH*, 1.7-fold), and the three glycogen synthases were slightly upregulated by 1.2- to 1.5-fold. Contrarily, genes involved in the amino acid anabolic pathway were not significantly changed. These results indicated that the accelerated rate of glucose utilization contributed to a shorter fermentation period and carbon source diversion, leading to the decrease in L-threonine production. In contrast, in ΔlsrB, CSG family gene expression was downregulated 0.2- to 0.4-fold, *fimA* and *fimH* expression was also downregulated 0.5-fold, *glgA* and *glgP* expression by 0.5-fold and 0.4-fold, respectively, and *glg*C was not significantly changed, which resulted in an increased fermentation period compared to *E. coli* W1688. Genes related to methionine metabolism were also downregulated, with no significant changes in *thrA*, *thrB*, and *thrC* expression. These results suggest that ΔlsrB did not change L-threonine production in *E. coli*.

In +plsrK, the expression of *glgA*, *glgP*, and *glgC* were reduced, which led to a decline in glucose utilization rate and a prolonged fermentation period. Likewise, the expression of *thrA*, *thrB*, and *thrC* were slightly reduced, affecting L-threonine production.

In ΔlsrR, the expression of *luxS* and *lsrB* were upregulated by 1.8-fold and 2.2-fold, respectively, and the expression of *lsrK* was upregulated by 7-fold. Meanwhile, the expression of CSG genes and glycogen synthases (*glgA* and *glgP*) were downregulated. The overexpression of LsrACDB operon and LsrK may have affected the consumption of the carbon source, contributing to the reduced fermentation yield of L-threonine. In contrast, in +plsrR, the reduced expression of *glgP* and *glgA* affected glycogen synthesis, possibly leading to a prolonged fermentation period.

2.7. Immobilized Repeated-Batch Fermentation in +pluxS and +plsrB

The results presented above showed a rise in biofilm formation and shorter fermentation period in +pluxS and +plsrB. Therefore, we performed immobilized continuous fermentation using these two mutants, with *E. coli* W1688 as a control strain. The results of the continuous fermentation of *E. coli* W1688, +pluxS, and +plsrB are shown in Figure 8A–C, respectively. In *E. coli* W1688, L-threonine production in the first batch was 10.05 g/L, and the fermentation period was 36 h. The second batch of fermentation yielded 10.51 g/L L-threonine in 34 h. The L-threonine production and fermentation periods remained stable in the third and fourth batches. In the fifth batch, the L-threonine yield was 11.34 g/L, while the fermentation period was shortened to 33 h. The seventh batch showed a significant gain in fermentation efficiency compared to the first batch (Batch 1: 10.05 g/L; Batch 7: 11.52 g/L) and exhibited a shorter fermentation period (Batch 1: 36 h; Batch 7: 32 h). Thus, the immobilized continuous fermentation of *E. coli* W1688 increased the L-threonine yield by 13.38%, and the fermentation period was shortened, indicating that the biofilm-immobilized fermentation strategy could improve the production of L-threonine and the production efficiency. With +pluxS, L-threonine production in the first batch was 9.32 g/L, and the fermentation period was 30 h. Similar to *E. coli* W1688, the set-up was prolonged until the seventh batch of fermentation. The production of L-threonine gradually increased and remained stable in the last two batches. Finally, the production of L-threonine reached 15.27 g/L, and the fermentation period was shortened to 28 h in the last batch. We also found that the highest yield of L-threonine in +pluxS using immobilized fermentation was 71.18% higher than that in the free-cell fermentation in +pluxS, and was 50.29% higher than that of *E. coli* W1688 free-cell fermentation, suggesting that +pluxS had more efficient fermentative production of L-threonine compared with *E. coli* W1688.

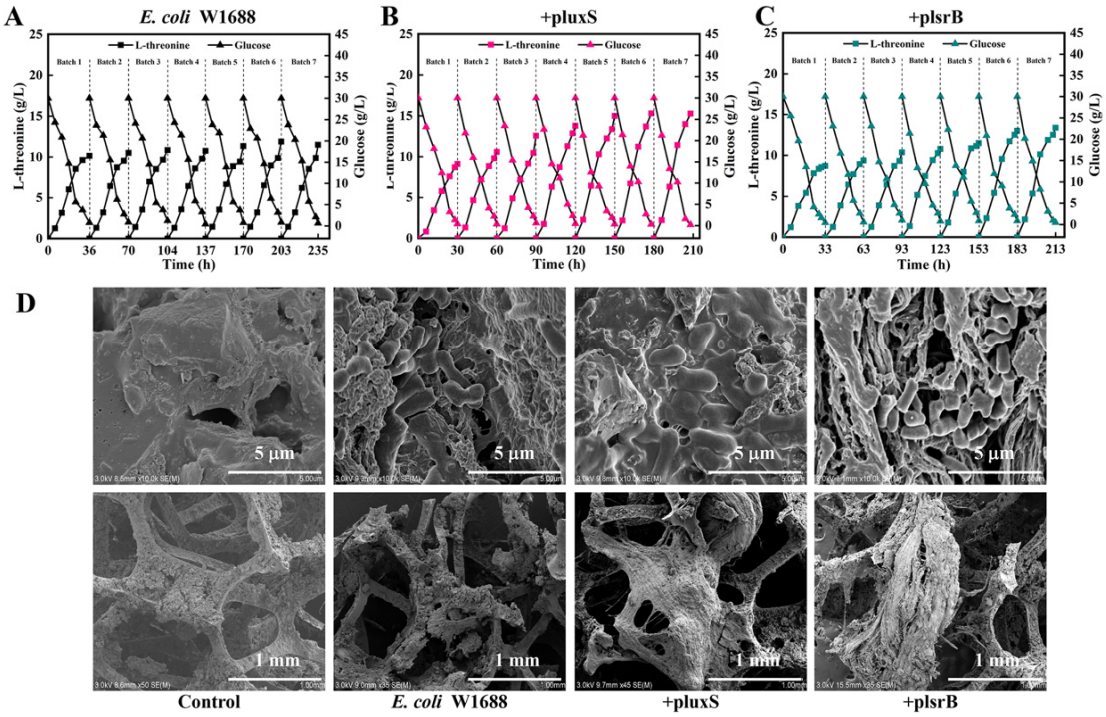

Figure 8. L-threonine production, glucose consumption, and SEM in immobilized continuous fermentation by *E. coli* W1688, +pluxS, and +plsrB. Immobilized continuous fermentation results of (**A**) *E. coli* W1688, (**B**) +pluxS, and (**C**) +plsrB. (**D**) SEM images of carrier in the immobilized fermentations of *E. coli* W1688, +pluxS, and +plsrB mutants using empty carrier as control.

With +plsrB, the first batch of fermentation yielded 8.72 g/L L-threonine, and the fermentation period was 33 h, which was not much different from that in the free-cell fermentation. In the second batch, the yield did not enhance significantly, but the fermentation period was shortened from 33 h to 30 h. Then, the fermentation period of succeeding batches were stable at 30 h, and the L-threonine yield increased from the third batch until the sixth and seventh batches. The final fermentation yield was 13.38 g/L, which was higher than that obtained in free-cell fermentation. Compared with the free-cell fermentation of *E. coli* W1688, the yield increased by 31.69%. These results demonstrate that modulating the AI-2 QS is an effective strategy to increase the yield of L-threonine and reduce the fermentation period during immobilized continuous fermentation. As shown in Table 1, overexpression of *luxS* also presents certain advantages compared to the L-threonine production of industrial *E. coli* strains in recent years. In terms of the yield of free-cell fermentation list in Table 1, the yield of *E. coli* W1688+pluxS reached the highest to 0.545 g/L/h and its conversion rate also presented obvious advantage.

Table 1. Comparison of L-threonine production using different engineered *E. coli* strains.

Strain	Time (h)	L-Threonine (g/L)	Productivity (g/L/h)	Conversion Rate (g/g)	Reference
Batch/shake-flash					
E. coli W1688	36	10.16	0.282	0.339	This study
E. coli W1688+pluxS	28	15.27	0.545	0.509	This study
E. coli W1688+plsrB	30	13.38	0.446	0.446	This study
E. coli TWF006/pFW01	36	15.9	0.44	0.53	[35]
E. coli βIM4	72	13.4	0.186	0.447	[36]
Fed-batch					
E. coli TH28C	50	82.4	1.648	0.393	[37]
E. coli EC125	48	105.3	2.194	0.405	[38]
E. coli THPE5	40	70.8	1.77	0.404	[39]

2.8. SEM Analysis of Biofilm on Carrier

To analyse whether AI-2 QS could regulate biofilm formation on the carrier during the immobilized fermentation, we observed the corresponding carriers using SEM (Figure 8D). Compared to an empty carrier used as control, a biofilm was formed on the carrier during the immobilized fermentation process of *E. coli* W1688, and +pluxS and +plsrB strains formed more extensive biofilms on the carrier. Notably, in the SEM image, it was observed that +pluxS and +plsrB had a block structure of biofilm, while that of *E. coli* W1688 was not obvious.

3. Discussion

Studies on *E. coli* biofilms are mainly focused on their roles and applications in clinical and environmental fields. In the clinical field, the removal of biofilms is necessary owing to their pathogenicity and drug resistance. Meanwhile, it is necessary to introduce the high resistance and activity of the biofilm in the industrial field. However, as an important platform strain in industrial production, studies on biofilm formation in *E. coli* in relation to industrial fermentation are relatively lacking. Biofilm formation is essential to improve fermentation efficiency; thus, methods that promote the formation of biofilm and improve the rate of biofilm formation are necessary. Currently, researchers aim to analyse the mechanisms underlying biofilm formation in *E. coli* and develop new targets to prevent and resolve infection and pollution. Among them, quorum sensing, which is the mode of communication between cells to form biofilms, has been a research hotspot in recent years. Therefore, this study aimed to highlight the role of AI-2 QS in regulating *E. coli* intraspecies communication, subsequently targeting biofilm formation, and understanding its role in industrial production.

MP Delisa et al. reported that the AI-2 signalling level was linearly related to the accumulation level of protein product [40]. The high expression of AI-2 may be a regulatory factor that promotes the production of metabolites. To investigate the effect of AI-2 QS system on the biofilm formation of industrial L-threonine producing *E. coli* W1688, we knocked out or overexpressed the four key genes (*luxS*, *lsrB*, *lsrK* and *lsrR*) in AI-2 QS system to generate eight mutant strains. Then, we verified the biofilm formation ability of all mutants through CV staining assay, motility assay, SEM, and fluorescence microscopy. We found that among the mutants, *luxS* and *lsrB* exert a greater influence on biofilm formation in *E. coli* W1688. Since curli formation and motility in *E. coli* are closely linked to biofilm formation [41], we also analysed the growth of curli fibres on YESCA-CR plates and the motility of colonies on 0.3% Eiken agar plates. The growth phenotypes further confirmed that the crucial influence of *luxS* and *lsrB* on *E. coli* W1688 biofilm formation. Previous studies in our laboratory have shown that promoting biofilm formation in *E. coli* is a key factor in enhancing immobilized fermentation [8]. Therefore, we analysed the fermentation performance of +pluxS and +plsrB as free cells and biofilm for the production of L-threonine. Surprisingly, both +plsrB and +pluxS gave lower L-threonine yields than *E. coli* W1688 in free-cell fermentation; however, the fermentation periods were reduced by 3 h and 6 h, respectively. Our preliminary analysis revealed that *luxS* overexpression could have affected the metabolic pathway of L-threonine biosynthesis, resulting in a reduced yield. In contrast, after *lsrB* overexpression, although L-threonine metabolism was not markedly affected, the increased expression of curli- and motility-related genes may have been responsible for reduced L-threonine production. The high expression level of glycogen synthase in both +pluxS and +plsrB indicates accelerated glucose utilization, which is probably responsible for the shortened fermentation period. In the context of immobilized fermentation, a comparative analysis was conducted between the immobilized fermentation of *E. coli* W1688 and that of +pluxS and +plsrB strains. After a span of seven batches, it was observed that the L-threonine yield exhibited an increase of 50.29% and 31.69% for the +pluxS and +plsrB strains, respectively. In addition, it was observed that the yields for +pluxS and +plsrB increased by 71.18% and 51.52%, respectively, in comparison to free fermentation. This highlights the benefits associated with the utilization of +pluxS and

+plsrB in facilitating the process of biofilm development. Furthermore, it is noteworthy to mention that the fermentation duration for +pluxS and +plsrB was comparatively shorter in comparison to that of *E. coli* W1688. Based on these results, we also considered whether the simultaneous overexpression of *luxS* and *lsrB* can achieve better fermentation yields. However, we found that the ability of such a strain to produce L-threonine was significantly weaker than *E. coli* W1688 (data not shown); therefore, this should be elucidated in future studies. In our study, we have presented in detail the role of the AI-2 QS system in biofilm formation and developed an immobilized continuous fermentation process for L-threonine production in *E. coli*. Several other mechanisms underlying bacterial communication occur in nature, such as AIP in Gram-positive bacteria, AHL in Gram-negative bacteria, the AI-3 QS system in enterohemorrhagic *E. coli* [42,43], and other undiscovered signalling molecules. These are potential biofilm regulation mechanisms for industrial strains and have the latent capacity to be applied to immobilized continuous fermentation.

4. Materials and Methods

4.1. Media and Growth Conditions

The bacterial strains, plasmids and growth conditions used in this study are listed in Table 2. *E. coli* W1688 (CCTCC M2015233), obtained from mutated *E. coli* MG1655 (ATCC47076), is an L-threonine producer that has a weak ability to form biofilms. *E. coli* W1688 and mutants were cultured in Luria–Bertani (LB) medium (10 g/L tryptone, 5 g/L yeast extract, 10 g/L NaCl) at 37 °C. The fermentation medium contained 30 g/L glucose, 2 g/L yeast extract, 1 g/L KH_2PO_4, 20 g/L $(NH_4)_2SO_4$, 0.8 g/L $MgSO_4{\cdot}7H_2O$, 0.2 g/L $FeSO_4{\cdot}7H_2O$, 0.2 g/L $MnSO_4{\cdot}5H_2O$, and 15 g/L $CaCO_3$. When necessary, 50 μg/mL kanamycin or 40 μg/mL streptomycin was added in LB medium to screen the *E. coli* transformants. Isopropyl-β-D-thiogalactoside (IPTG, 0.5 mM) was added to induce expression in strains containing the plasmid pET28a. L-arabinose (30 mM) was used to induce pCAS expression during CRISPR/Cas9 gene editing.

Table 2. Strains and plasmids used in this study.

Strains/Plasmids	Relevant Characteristics	Culture Temperature	Sources
Strains			
E. coli W1688	L-threonine producing strain	37 °C	Stored in our lab
⊗luxS	*E. coli* W1688 with the deletion of *luxS*	37 °C	This study
⊗lsrB	*E. coli* W1688 with the deletion of *lsrB*	37 °C	This study
⊗lsrK	*E. coli* W1688 with the deletion of *lsrK*	37 °C	This study
⊗lsrR	*E. coli* W1688 with the deletion of *lsrR*	37 °C	This study
+pluxS	*E. coli* W1688 harbouring plasmid pET28a-*luxS*	37 °C	This study
+plsrB	*E. coli* W1688 harbouring plasmid pET28a-*lsrB*	37 °C	This study
+plsrK	*E. coli* W1688 harbouring plasmid pET28a-*lsrK*	37 °C	This study
+plsrR	*E. coli* W1688 harbouring plasmid pET28a-*lsrR*	37 °C	This study
V. harveyi BB170	BB120luxN:Tn5 (sensor 1-, sensor 2+)	30 °C	[44]
Plasmids			
pET28a	Kan resistance	37 °C	Stored in our lab
pCas	Kan resistance	30 °C	[45]
pTarget	Streptomycin resistance	37 °C	[45]

4.2. Construction of luxS, lsrB, lsrK, and lsrR Mutants

The ΔluxS, ΔlsrB, ΔlsrK, and ΔlsrR mutant strains were obtained by knocking out the target genes in *E. coli* W1688 using CRISPR/Cas9 gene editing technology [46]. Briefly, a 20 bp sequence from the target gene was selected to construct the pTarget plasmid. Then, the plasmid and repaired donor DNA were introduced into the competent *E. coli* W1688 containing the pCas plasmid. The transformed cells were screened to obtain the target gene deletion strain. Kanamycin and streptomycin resistance were used as selection markers to obtain the ΔluxS strain. The ΔlsrB, ΔlsrK, and ΔlsrR strains were obtained using the same gene knockout method.

The *luxS*, *lsrB*, *lsrK*, and *lsrR* genes were amplified from the genome of *E. coli* W1668 using the corresponding primers (Table 3). The PCR products were digested using the restriction enzymes *Nco I* and *XhoI* and ligated into the *NcoI*/*XhoI*-digested vector pET28a using the ClonExpress II one step cloning kit C112-01 (Vazyme, Nanjing, China). The constructed plasmids were transformed into *E. coli* W1668 using an electroporation system at 2.5 kV, 25 mF, and 200 Ω. Kanamycin (50 μg/mL) was used to screen the transformants.

Table 3. Sequence of the oligonucleotide primers used in this study.

Primer Name	Primer Sequence (5′ to 3′)
luxS-sg-F	TGTTGCTGATGCCTGGAAAGGTTTTAGAGCTAGAAATAGCAAGTTAAAATAAGGCTAGT
luxS-sg-R	CTTTCCAGGCATCAGCAACAACTAGTATTATACCTAGGACTGAGCTAGCTG
luxS-up-F	GGAACCGGGTGATCCTCGA
luxS-up-R	GTGCAGTTCCTGCGCTATCTAACAACGGCATTTAGCCAC
luxS-dn-F	TTGTTAGATAGCGCAGGAACTGCACATCTAGTCAG
luxS-dn-R	CCGTCTGCTTCTACTGGCG
lsrB-sg-F	TGGTGTGAGAGTGCTGACCTGTTTTAGAGCTAGAAATAGCAAGTTAAAATAAGGCTAGT
lsrB-sg-R	AGGTCAGCACTCTCACACCAACTAGTATTATACCTAGGACTGAGCTAGCTG
lsrB-up-F	CTGGCTCTGGCTGCATAAAAC
lsrB-up-R	CGCTCCGGGAGCGCTAAGTAAGGCGATTTTCT
lsrB-dn-F	AGCGCTCCCGGAGCGCGTGATATTCAAC
lsrB-dn-R	CCGATATAAACCTGCGCCGC
lsrK-sg-F	TGGCTGGCCTATATGCTCAGGTTTTAGAGCTAGAAATAGCAAGTTAAAATAAGGCT
lsrK-sg-R	CTGAGCATATAGGCCAGCCAACTAGTATTATACCTAGGACTGAGCTAGCTG
lsrK-up-F	GCAGCGGATGTGGCGA
lsrK-up-R	CTGATCCTGCCGGTGCCTGCATCC
lsrK-dn-F	AGGCACCGGCAGGATCAGCTGGGGCT
lsrK-dn-R	GTGTTAGTTGGAGGTGGGAAGGT
lsrR-sg-F	GGGAATCGGGCAGCTTAACGGTTTTAGAGCTAGAAATAGCAAGTTAAAATAAGGCT
lsrR-sg-R	CGTTAAGCTGCCCGATTCCCACTAGTATTATACCTAGGACTGAGCTAGCTG
lsrR-up-F	TTGGGAAAAGCAGCGGTTCCT
lsrR-up-R	TGCAGCGGCGTCGTGATAGTAAAACCACGCG
lsrR-dn-F	TCACGACGCCGCTGCAATGAAAGGC
lsrR-dn-R	GTTCGCTAACTTCGCGTGCC
luxS-F	AGGAGATATACCATGCCGTTGTTAGATAGCTTCACAG
luxS-R	GGTGGTGGTGCTCGAGGATGTGCAGTTCCTGCAACTTCT
lsrB-F	AGGAGATATACCATGACACTTCATCGCTTTAAGAAAATCGC
lsrB-R	GGTGGTGGTGCTCGAGGAAATCGTATTTGCCGATATTCTCTTTGTTGAA
lsrK-F	AGGAGATATACCATGGCTCGACTCTTTACCCTTTCAG
lsrK-R	GGTGGTGGTGCTCGAGTAACCCAGGCGCTTTCCATAACGAC
lsrR-F	AGGAGATATACCATGATGACAATCAACGATTCGGCAAT
lsrR-R	GGTGGTGGTGCTCGAGACTACGTAAAATCGCCGCTG

4.3. Growth Curves

Overnight cultures of the different strains were diluted to obtain an OD_{600} of 0.1 and then inoculated into fresh LB medium. At 2, 4, 6, 8, 10, 12, and 14 h, the cell densities at OD_{600} were measured using a microplate reader. The experiment was performed three times.

4.4. Biofilm Forming Capacity

Crystal violet (CV) staining was used to quantify biofilm formation of the different *E. coli* mutants [46]. Briefly, overnight cultures in fermentation medium were diluted to obtain an OD_{600} of 0.1. Then, 200 μL of diluted culture was transferred to 96-well plates (Corning, NY, USA) and incubated at 37 °C for 36 h. The wells were washed gently with 1% phosphate-buffered saline (PBS) to remove free cells. To fix the biofilms, glutaraldehyde (2.5%) was added for 20 min at 4 °C, and then the biofilms were stained with 1% CV for 20 min, washed with PBS, and air-dried. For quantification, 200 μL acetic acid was added

to each well to dissolve the crystal violet, with slow shaking for 20 min. The absorbance was measured at 570 nm using a microplate reader.

Following a previously described method [8], fluorescence microscopy was used to visualize adhesion properties of the bacteria and distribution of cells in biofilms. *E. coli* W1688 cells were stained with 4′,6-diamidino-2-phenylindole (DAPI) (Sigma, St. Louis, MO, USA) and viewed directly under a fluorescence microscope. Scanning electron microscopy (SEM) was also used to observe biofilms. Briefly, sterile round coverslips were placed in 12-well plates, then 4 mL of fermentation broth and 40 μL of different dilutions of bacterial broth were added in each well and incubated at 37 °C for 30 h. At the end of incubation, the free bacteria were gently removed and washed with sterile PBS, and then the biofilms were scraped off the round coverslips in sheets with a needle, dehydrated in an ethanol gradient (25%, 50%, 75%, 95%, and 100% for 10 min each), and finally soaked in tert-butanol for 10 min. The resulting mixture was centrifuged (5000× *g* at 4 °C for 5 min) to remove the tert-butanol and frozen overnight at −80 °C. Biofilm cells were dried using a FreeZone® 4.5 L Freeze Dry System (Labconco, Kansas City, MO, USA) and sputter-coated with gold. Images were acquired by using SEM (SEM 4800, Hitachi, Tokyo, Japan).

4.5. Curli Stain on YESCA-CR Plates

When grown on plates supplemented with congo red (CR), curli fibres of *E. coli* can be stained red, providing a convenient way to identify genes involved in curli expression [47]. Briefly, 2.5 μL of overnight cultures were inoculated on YESCA-CR plates, incubated at 30 °C for 48 h, and then photographed for recording. YESCA-CR plates contained 1 g/L yeast extract, 10 g/L casamino acids, and 20 g/L agar. Sterile CR (50 μg/mL) and brilliant blue (1 μg/mL) were added after autoclave sterilization of YESCA.

4.6. Motility Assay

Overnight cultures of the different strains were grown in LB medium, and then 2.5 μL of each culture was inoculated on swarming plates. The swarming motility plates contained 0.3% Eiken agar (Eiken Chemical, Tokyo, Japan), 1% tryptone, 0.5% yeast extract, 0.5% NaCl, and 0.3% glucose. The plates were dried for 3–4 h before inoculation. Then, the cultures were inoculated and photographed after 16 h incubation at 30 °C. When the assays were performed using the strains carrying pET28a, the plates also contained kanamycin.

4.7. AI-2 Detection

Vibrio harveyi BB170 cells were used to measure AI-2 activity following the method described previously [44]. Briefly, the different strains were centrifuged at 12,000× *g* at 4 °C for 10 min, and the cell-free culture fluid (CF) was obtained using filtration through 0.22 mm filter and frozen at −80 °C. *V. harveyi* BB170 was diluted (1:5000) in autoinducer bioassay medium [48], and each CF sample was added to the diluted *V. harveyi* BB170 culture at 1:9 ratio. The mixture was incubated at 28 °C for 5 h. The CFs from *V. harveyi* BB170 and *E. coli* DH5α were used as the positive and negative controls, respectively. Aliquots (200 μL) were added to black 96-well plates to detect luminescence values using a multiscan spectrum in luminescence mode (SpectraMax iD5; Molecular Devices; San Jose, CA, USA). The experiment was performed in triplicates.

4.8. qRT-PCR Analysis

The analysed genes and primers used in the analysis are listed in Table 4. Briefly, *E. coli* cells at logarithmic phase in the fermentation medium were collected, washed twice with PBS, and then centrifuged to obtain samples for RNA extraction. Total RNA was extracted using RNAprep Pure Cell/Bacteria Kit (TianGen Biotech, Beijing, China) according to the manufacturer's instructions. Reverse transcription was performed using the HiScript® III RT SuperMix for qRT-PCR (+gDNA wiper) (Vazyme). After reverse transcription, cDNAs were prepared for qRT-PCR. SYBR qRT-PCR Master Mix (Vazyme) was used for qRT-PCR in a StepOnePlus Real-Time PCR System (Applied Biosystems, Waltham, MA, USA). The

16S rRNA gene was used as an endogenous control to normalize the target, and gene transcription levels were determined according to the $2^{-\otimes\otimes Ct}$ method.

Table 4. Genes and primers used for qRT-PCR.

Gene	Forward Primer Sequence (5′-3′)	Reverse Primer Sequence (5′-3′)
luxS	GAACGTCTACCAGTGTGGCA	GTGCCAGTTCTTCGTTGCTG
lsrB	ATACTAAACCGGAGTGCCGC	AACGCGACTTTGGCTTTGTC
lsrK	TGGCCTACGTGCCGATATTC	TTGTGAACTTACCACGCCCA
lsrR	ATTGGTTTTGGCGAGGCAAC	TATAAGAACCGACGCCACCG
fimA	GGCAATCGTTGTTCTGTCGG	TCCCACCATTAACCGTCGTG
fimH	GATGCGGGCAACTCGATT	CGCCCTGTGCAGGTGAA
flhD	CGTCTGGTGGCTGTCAAAAC	CGTTAGCGGCACTGACTCTT
flhC	GCTTGTGGGCACTGTTCAAG	CCGGTTTGTGTAATGGCGTC
csgA	AGTACGGTGGCGGTAACTCT	TGTCATCTGAGCCCTGACCA
csgB	TAGTGCTCAGTTACGGCAGG	TGGTCAATCTTTGCCCGGTT
csgC	TTCAGGGCAAAGTCAGACGA	TAGCAGGCAATGAAAGGGTCT
csgD	CGTAAAGTAGCATTCGCCGC	GATTACCCGTACCGCGACAT
flu	ACGGTAAATGGCGGACTGTT	CACGGATGGTCAGGGTATCG
wza	CCCGCAGGTGGACGTTAATA	TAGTCAGTGGCACGTTGGTG
glgA	CAAAGACAAACCCACTGGCG	TGGGCTTGCTGATACGGTTT
glgP	AGTGCAGTTCCGATACACCG	GATACCGATCTGCTGGGACG
glgC	CATAACGCCAAATGCGGAGG	GCGGGCGACCATATCTACAA
thrA	CTTCACCCCCGCACCAT	ATCAGGCAAGGGATCTGGAA
thrB	CGAGCTGGAAGGCCGTATC	AACACGGTGCCACGTTGTC
thrC	AAGCGACTCAGGCGACGTTA	CACACGCGGCCAGTTGT
lysC	GCACAGCCTGAATATGCTGC	GCGAGGATGCCGAAAACTTC
rhtA	TCGTCGCCCGGTAGATTTC	GCAGGAACCACAGACCAAGAA
metB	CCCGGCATTACAAAATCCGC	GAATGCAACACCAGATCGGC
metC	ACTCTCGGCGCGGTAAATAG	CAAAGACCAGCGAAGAAGCG
metH	GTCAACGATCCGGCATTTCG	CGCTTTGGTGGACTCTCGAT
metL	TACACGCCGGATCAAGGTTC	GACATCATCGTGGCTGGTGA
16S rna	TCGGGAACCGTGAGACAGG	CCGCTGGCAACAAAGGATAAG

4.9. Free-Cell Fermentation, Immobilized Fermentation, and SEM

For free-cell fermentation, the supernatant was used to quantify L-threonine and residual sugars using high-performance liquid chromatography. For immobilized continuous fermentation, 30 g/L of carrier (a polymer porous foam consisting of polyurethane and carbon black) used in fermentation was prepared according to a previous study [10]. Briefly, 80% of the fermentation broth was removed after the first batch, and the remaining 20% with carrier covered with the biofilm was reserved for the next batch. After adding fresh medium, the second batch was initiated under the same conditions as above until the titre of L-threonine was stable. Subsequent batches were operated as described [8].

Subsequently, the immobilized carrier with biofilm cells was harvested after fermentation and treated as described above. Images were acquired using SEM (SEM 4800, Hitachi, Japan).

L-threonine concentrations were measured using high-performance liquid chromatography (Agilent 1260 series; Hewlett-Packard, Palo Alto, CA, USA) with a UV detector, using a Sepax AAA ion exclusion column (250 × 4.6 mm; Bio-Rad Laboratories, Hercules, CA, USA), with 0.1 M sodium acetate and 80% acetonitrile as the mobile phase (1 mL/min) at 36 °C [8]. Before sample detection, 200 μL of the sample solution was transferred into a 1.5 mL plastic tube. Next, 100 μL of triethylamine solution and 100 μL of phenyl isothiocyanate solution were added to the tube. These components were mixed thoroughly. After allowing the mixture to react at room temperature for 1 h, 400 μL of n-hexane was added. Vortex oscillation was performed for 10 min. The mixture was left to stand for 30 min, then the phase was remove and filtered using a 0.45 μm filter membrane before taking the sample.

4.10. Statistical Analysis

All experiments were conducted at least in triplicates. Statistical significance was analysed using one- or two-way analysis of variance (ANOVA) or paired *t*-test with Prism software (GraphPad Prism 9.5.1 software, San Diego, CA, USA). Data are reported as the means and standard deviations of three independent experiments. p values were computed using Student's t test (n.s., not significant at $p > 0.05$; *** $p < 0.001$; ** $p < 0.01$; and * $p < 0.05$).

5. Conclusions

In conclusion, we found that in *E. coli* AI-2 QS, *luxS*, and *lsrB* played a significant role in regulating AI-2 and biofilm formation. Moreover, *luxS* and *lsrB* can regulate motility and curli formation. We obtained two enhanced biofilm-forming strains by expressing *luxS* and *lsrB* and utilized them for immobilized continuous fermentations, where +pluxS showed significant results in terms of increased L-threonine production and a shortened fermentation period. Therefore, immobilized continuous fermentation may be an effective method to improve the production of bioenergy or bio-based chemicals by industrial *E. coli*. Our study also provides a reference value for the QS system in the efficient biofilm production of other industrial microorganisms.

Author Contributions: Conceptualization, Y.C. and W.S.; methodology, Y.Y.; validation, T.C., P.Y. and H.N.; data curation, S.S., C.L. and K.Z.; writing—original draft preparation, Y.Y. and G.L.; writing—review and editing, H.H. and W.S.; funding acquisition, Y.C., W.Z. and D.L. All authors have read and agreed to the published version of the manuscript.

Funding: This work was supported by the National Key R&D Program of China (Grant No. 2022YFC2105400; Grant No. 2021YFC2101100; Grant No. 2022YFC2104600); the National Natural Science Foundation of China (Grant No. 22178176; Grant No. 22208157); Jiangsu National Synergetic Innovation Center for Advanced Materials (SICAM); Key Research and Development Program of Nanjing Jiangbei New Area (Grant No. ZDYF20200220); Key R&D plan of Jiangsu Province (Grant No. BE2019001); and the Youth Fund of Natural Science Foundation of Jiangsu Province (Grant No. BK20220334).

Institutional Review Board Statement: Not applicable.

Informed Consent Statement: Not applicable.

Data Availability Statement: Not applicable.

Conflicts of Interest: The authors declare no conflict of interest.

References

1. Fang, K.; Jin, X.; Hong, S.H. Probiotic *Escherichia coli* inhibits biofilm formation of pathogenic *E. coli* via extracellular activity of DegP. *Sci. Rep.* **2018**, *8*, 4939. [CrossRef]
2. Miquel, S.; Lagrafeuille, R.; Souweine, B.; Forestier, C. Anti-biofilm activity as a health issue. *Front. Microbiol.* **2016**, *7*, 592. [CrossRef]
3. Hall, C.W.; Mah, T.-F. Molecular mechanisms of biofilm-based antibiotic resistance and tolerance in pathogenic bacteria. *FEMS Microbiol. Rev.* **2017**, *41*, 276–301. [CrossRef]
4. Sharma, G.; Sharma, S.; Sharma, P.; Chandola, D.; Dang, S.; Gupta, S.; Gabrani, R. *Escherichia coli* biofilm: Development and therapeutic strategies. *J. Appl. Microbiol.* **2016**, *121*, 309–319. [CrossRef]
5. Lister, J.L.; Horswill, A.R. Staphylococcus aureus biofilms: Recent developments in biofilm dispersal. *Front. Cell Infect. Microbiol.* **2014**, *4*, 178. [CrossRef] [PubMed]
6. Flemming, H.-C.; Wingender, J.; Szewzyk, U.; Steinberg, P.; Rice, S.A.; Kjelleberg, S. Biofilms: An emergent form of bacterial life. *Nat. Rev. Microbiol.* **2016**, *14*, 563–575. [CrossRef] [PubMed]
7. Jiang, Y.; Liu, Y.; Zhang, X.; Gao, H.; Mou, L.; Wu, M.; Zhang, W.; Xin, F.; Jiang, M. Biofilm application in the microbial biochemicals production process. *Biotechnol. Adv.* **2021**, *48*, 107724. [CrossRef]
8. Chen, T.; Liu, N.; Ren, P.; Xi, X.; Yang, L.; Sun, W.; Yu, B.; Ying, H.; Ouyang, P.; Liu, D.; et al. Efficient Biofilm-Based Fermentation Strategies for L-Threonine Production by *Escherichia coli*. *Front. Microbiol.* **2019**, *10*, 1773. [CrossRef]
9. Yang, L.; Zheng, C.; Chen, Y.; Shi, X.; Ying, Z.; Ying, H. Nitric oxide increases biofilm formation in *Saccharomyces cerevisiae* by activating the transcriptional factor Mac1p and thereby regulating the transmembrane protein Ctr1. *Biotechnol. Biofuels* **2019**, *12*, 30. [CrossRef]

10. Yu, B.; Zhang, X.; Sun, W.; Xi, X.; Zhao, N.; Huang, Z.; Ying, Z.; Liu, L.; Liu, D.; Niu, H.; et al. Continuous citric acid production in repeated-fed batch fermentation by *Aspergillus niger* immobilized on a new porous foam. *J. Biotechnol.* **2018**, *276*, 1–9. [CrossRef] [PubMed]
11. Liu, D.; Chen, Y.; Li, A.; Ding, F.; Zhou, T.; He, Y.; Li, B.; Niu, H.; Lin, X.; Xie, J.; et al. Enhanced butanol production by modulation of electron flow in *Clostridium acetobutylicum* B3 immobilized by surface adsorption. *Bioresour. Technol.* **2013**, *129*, 321–328. [CrossRef] [PubMed]
12. Sun, W.; Shi, S.; Chen, J.; Zhao, W.; Chen, T.; Li, G.; Zhang, K.; Yu, B.; Liu, D.; Chen, Y.; et al. Blue Light Signaling Regulates Escherichia coli W1688 Biofilm Formation and l-Threonine Production. *Microbiol. Spectr.* **2022**, *10*, e0246022. [CrossRef]
13. Berlanga, M.; Guerrero, R. Living together in biofilms: The microbial cell factory and its biotechnological implications. *Microb. Cell Fact.* **2016**, *15*, 165. [CrossRef]
14. Pan, Y.; Breidt, F., Jr.; Gorski, L. Synergistic effects of sodium chloride, glucose, and temperature on biofilm formation by *Listeria monocytogenes* serotype 1/2a and 4b strains. *Appl. Environ. Microbiol.* **2010**, *76*, 1433–1441. [CrossRef] [PubMed]
15. Liu, L.; Yu, B.; Sun, W.; Liang, C.; Ying, H.; Zhou, S.; Niu, H.; Wang, Y.; Liu, D.; Chen, Y. Calcineurin signaling pathway influences *Aspergillus niger* biofilm formation by affecting hydrophobicity and cell wall integrity. *Biotechnol. Biofuels* **2020**, *13*, 1–13. [CrossRef] [PubMed]
16. Rutherford, S.T.; Bassler, B.L. Bacterial quorum sensing: Its role in virulence and possibilities for its control. *Cold Spring Harb. Perspect. Med.* **2012**, *2*, a012427. [CrossRef] [PubMed]
17. Waters, C.M.; Bassler, B.L. Quorum sensing: Cell-to-cell communication in bacteria. *Annu. Rev. Cell Dev. Biol.* **2005**, *21*, 319–346. [CrossRef] [PubMed]
18. Wang, Y.; Yi, L.; Zhang, Z.; Fan, H.; Cheng, X.; Lu, C. Overexpression of *luxS* cannot increase autoinducer-2 production, only affect the growth and biofilm formation in *Streptococcus suis*. *Sci. World J.* **2013**, *2013*, 924276. [CrossRef] [PubMed]
19. Wang, Y.; Wang, Y.; Sun, L.; Grenier, D.; Yi, L. The LuxS/AI-2 system of *Streptococcus suis*. *Appl. Microbiol. Biotechnol.* **2018**, *102*, 7231–7238. [CrossRef]
20. Brackman, G.; Coenye, T. Quorum sensing inhibitors as anti-biofilm agents. *Curr. Pharm. Des.* **2015**, *21*, 5–11. [CrossRef]
21. Banerjee, G.; Ray, A.K. Quorum-sensing network-associated gene regulation in Gram-positive bacteria. *Acta Microbiol. Immunol. Hung.* **2017**, *64*, 439–453. [CrossRef] [PubMed]
22. Smith, D.; Wang, J.H.; Swatton, J.E.; Davenport, P.; Price, B.; Mikkelsen, H.; Stickland, H.; Nishikawa, K.; Gardiol, N.; Spring, D.R.; et al. Variations on a theme: Diverse N-acyl homoserine lactone-mediated quorum sensing mechanisms in gram-negative bacteria. *Sci. Prog.* **2006**, *89*, 167–211. [CrossRef]
23. Xavier, K.B.; Bassler, B.L. Interference with AI-2-mediated bacterial cell–cell communication. *Nature* **2005**, *437*, 750–753. [CrossRef] [PubMed]
24. Li, J.; Attila, C.; Wang, L.; Wood, T.K.; Valdes, J.J.; Bentley, W.E. Quorum sensing in *Escherichia coli* is signaled by AI-2/LsrR: Effects on small RNA and biofilm architecture. *J. Bacteriol.* **2007**, *189*, 6011–6020. [CrossRef] [PubMed]
25. Pereira, C.S.; de Regt, A.K.; Brito, P.H.; Miller, S.T.; Xavier, K.B. Identification of functional LsrB-like autoinducer-2 receptors. *J. Bacteriol.* **2009**, *191*, 6975–6987. [CrossRef]
26. De Keersmaecker, S.C.; Sonck, K.; Vanderleyden, J. Let LuxS speak up in AI-2 signaling. *Trends Microbiol.* **2006**, *14*, 114–119. [CrossRef]
27. Schauder, S.; Shokat, K.; Surette, M.G.; Bassler, B.L. The LuxS family of bacterial autoinducers: Biosynthesis of a novel quorum-sensing signal molecule. *Mol. Microbiol.* **2001**, *41*, 463–476. [CrossRef]
28. Stephens, K.; Zargar, A.; Emamian, M.; Abutaleb, N.; Choi, E.; Quan, D.N.; Payne, G.; Bentley, W.E. Engineering *Escherichia coli* for enhanced sensitivity to the autoinducer-2 quorum sensing signal. *Biotechnol. Prog.* **2019**, *35*, e2881. [CrossRef]
29. Torres-Cerna, C.E.; Morales, J.A.; Hernandez-Vargas, E.A. Modeling quorum sensing dynamics and interference on *Escherichia coli*. *Front. Microbiol.* **2019**, *10*, 1835. [CrossRef]
30. Rezzonico, F.; Duffy, B. Lack of genomic evidence of AI-2 receptors suggests a non-quorum sensing role for luxS in most bacteria. *BMC Microbiol.* **2008**, *8*, 154. [CrossRef]
31. Laganenka, L.; Sourjik, V. Autoinducer 2-dependent Escherichia coli biofilm formation is enhanced in a dual-species coculture. *Appl. Environ. Microbiol.* **2018**, *84*, e02638-17. [CrossRef]
32. Kapuscinski, J. DAPI: A DNA-specific fluorescent probe. *Biotech. Histochem.* **1995**, *70*, 220–233. [CrossRef]
33. Partridge, J.D.; Nhu, N.T.; Dufour, Y.S.; Harshey, R.M. *Escherichia coli* remodels the chemotaxis pathway for swarming. *mBio* **2019**, *10*, e00316-19. [CrossRef] [PubMed]
34. Xavier, K.B.; Bassler, B.L. LuxS quorum sensing: More than just a numbers game. *Curr. Opin. Microbiol.* **2003**, *6*, 191–197. [CrossRef] [PubMed]
35. Zhao, H.; Fang, Y.; Wang, X.; Zhao, L.; Wang, J.; Li, Y. Increasing L-threonine production in *Escherichia coli* by engineering the glyoxylate shunt and the L-threonine biosynthesis pathway. *Appl. Microbiol. Biotechnol.* **2018**, *102*, 5505–5518. [CrossRef]
36. Miwa, K.; Tsuchida, T.; Kurahashi, O.; Nakamori, S.; Sano, K.; Momose, H. Construction of L-threonine overproducing strains of *Escherichia coli* K-12 using recombinant DNA techniques. *Agric. Biol. Chem.* **1983**, *47*, 2329–2334. [CrossRef]
37. Lee, K.H.; Park, J.H.; Kim, T.Y.; Kim, H.U.; Lee, S.Y. Systems metabolic engineering of *Escherichia coli* for L-threonine production. *Mol. Syst. Biol.* **2007**, *3*, 149. [CrossRef]

38. Liu, S.; Liang, Y.; Liu, Q.; Tao, T.; Lai, S.; Chen, N.; Wen, T. Development of a two-stage feeding strategy based on the kind and level of feeding nutrients for improving fed-batch production of l-threonine by *Escherichia coli*. *Appl. Microbiol. Biotechnol.* **2013**, *97*, 573–583. [CrossRef]
39. Liu, J.; Li, H.; Xiong, H.; Xie, X.; Chen, N.; Zhao, G.; Caiyin, Q.; Zhu, H.; Qiao, J. Two-stage carbon distribution and cofactor generation for improving L-threonine production of *Escherichia coli*. *Biotechnol. Bioeng.* **2019**, *116*, 110–120. [CrossRef]
40. DeLisa, M.P.; Valdes, J.J.; Bentley, W.E. Quorum signaling via AI-2 communicates the "Metabolic Burden" associated with heterologous protein production in *Escherichia coli*. *Biotechnol. Bioeng.* **2001**, *75*, 439–450. [CrossRef] [PubMed]
41. Pratt, L.A.; Kolter, R. Genetic analysis of *Escherichia coli* biofilm formation: Roles of flagella, motility, chemotaxis and type I pili. *Mol. Microbiol.* **1998**, *30*, 285–293. [CrossRef] [PubMed]
42. Walters, M.; Sircili, M.P.; Sperandio, V. AI-3 synthesis is not dependent on luxS in *Escherichia coli*. *J. Bacteriol.* **2006**, *188*, 5668–5681. [CrossRef]
43. Galloway, W.R.; Hodgkinson, J.T.; Bowden, S.D.; Welch, M.; Spring, D.R. Quorum sensing in Gram-negative bacteria: Small-molecule modulation of AHL and AI-2 quorum sensing pathways. *Chem. Rev.* **2011**, *111*, 28–67. [CrossRef]
44. Bassler, B.L.; Greenberg, E.P.; Stevens, A.M. Cross-species induction of luminescence in the quorum-sensing bacterium Vibrio harveyi. *J. Bacteriol.* **1997**, *179*, 4043–4045. [CrossRef]
45. Jiang, Y.; Chen, B.; Duan, C.; Sun, B.; Yang, J.; Yang, S. Multigene editing in the *Escherichia coli* genome via the CRISPR-Cas9 system. *Appl. Environ. Microbiol.* **2015**, *81*, 2506–2514. [CrossRef] [PubMed]
46. Liu, L.; Wu, R.; Zhang, J.; Li, P. Overexpression of luxS promotes stress resistance and biofilm formation of *Lactobacillus paraplantarum* L-ZS9 by regulating the expression of multiple genes. *Front. Microbiol.* **2018**, *9*, 2628. [CrossRef]
47. Collinson, S.; Doig, P.; Doran, J.; Clouthier, S.; Trust, T.; Kay, W. Thin, aggregative fimbriae mediate binding of *Salmonella enteritidis* to fibronectin. *J. Bacteriol.* **1993**, *175*, 12–18. [CrossRef]
48. Greenberg, E.; Hastings, J.W.; Ulitzur, S. Induction of luciferase synthesis in *Beneckea harveyi* by other marine bacteria. *Arch. Microbiol.* **1979**, *120*, 87–91. [CrossRef]